A Decision Support Tool for the Economic Impact Assessment of Structural Health Monitoring Systems in Composite Rotorcraft Elements

Pietro Ballarin, Department of Aerospace Science and Technology, Politecnico di Milano, Milan (MI), Italy
Giuseppe Sala, Department of Aerospace Science and Technology, Politecnico di Milano, Milan (MI), Italy
Marco Macchi, Department of Management Engineering, Politecnico di Milano, Milan (MI), Italy
Irene Roda, Department of Management Engineering, Politecnico di Milano, Milan (MI), Italy
Andrea Baldi, Leonardo Helicopters Division, Cascina Costa di Samarate (VA), Italy
Alessandro Airoldi, Department of Aerospace Science and Technology, Politecnico di Milano, Milan (MI), Italy

Abstract

Structural Health Monitoring Systems (SHMS) allow an on-line monitoring of the rotorcraft's structure, with the advantage to reduce the effort for maintenance. However, their impact on the lifecycle is still unclear. In this work, a methodology to assess the economic impact of SHMS is presented, and it is divided in four steps: (i) identification of SHMS application; (ii) SHMS performance assessment; (iii) integration of SHMS in the lifecycle; (iv) Economic impact assessment. Such methodology is applied to two different lifecycle stages of a composite rotorcraft blade: Beginning Of Life (BOL), concerning the development of a new sensorized element, and Middle Of Life (MOL), concerning the usage and maintenance of the component. It was found that in the BOL stage, SHMS can potentially provide economic benefits if the SHMS allows reducing the number of curing cycles and tested blades below a certain threshold. In the MOL, it was found that the saving of the manpower allowed by the SHMS is compensated by a higher cost of the spare parts, and the higher repairing time.

1. NOTATION

Symbols

$\ldots^{as\ is}$	Superscript referring to the scenario "as is"
$\ldots^{SHMS}$	Superscript referring to the scenario "with SHMS"
$C_{acq\ sys}$	Cost of the acquisition system for the scenario "as is"
c_{blade}	Cost of the blade to the customer
$C_{cur\ cycle\ def}$	Cost to define the curing cycle
C_{energy}	Cost of energy for the autoclave
CF	Cash flow per year
C_{FBG}	Cost of 1 FBG sensor
$C_{FBG\ sys}$	Cost of the interrogation system for FBG sensors
c_{fuel}	Cost of fuel per hour consumed by the helicopter
C_g	Cost of 1 strain gauge
$C_{lab\ act}$	Cost to perform laboratory activities
C_m	Cost of the material to produce one blade
$C_{test\ lab}$	Cost to perform laboratory tests
C_{th}	Cost of 1 thermocouple
$K_{partition}$	Partition coefficient between the time to perform the activities on the blade and the time to perform the activities on the whole helicopter
L_{eng}	Labor rate of engineers
L_{pilots}	Labor rate of pilots
$L_{tr\ wo}$	Labor rate of trained workers
n_{auto}	Number of autoclave cycles

n_b	Number of rotor blades
n_{FBG}	Number of FBG sensors embedded in one blade
n_g	Number of strain gauges applied on one blade
n_{test}	Number of laboratory blade tests
n_{th}	Number of thermocouples embedded in one blade
R	Revenue loss
r	Discount rate
t_{auto}	Time to perform one autoclave cycle
t_{depot}	Time needed by the helicopter to reach the depot
t_{DI}	Time to perform detailed inspection
t_{eng}	Time needed by the engineers to assess the quality of the acquired data
t_{GVI}	Time to perform general visual inspection
$t_{mount\ blade}$	Time to mount/remove one blade on the rotor hub
t_{repair}	Time to repair one blade
t_{test}	Time to perform one test on the blade
$t_{tr\ wo}$	Time needed by the trained workers to laminate, prepare the vacuum bag and demould the blade

Acronyms:

ANN	Artificial Neural Network
BOL	Beginning Of Life
DAER-lab	Laboratory of the Department of Aerospace Science and Technology of Politecnico di Milano
DI	Detailed Inspection
DVI	Detailed Visual Inspection
EOL	End Of Life
FBG	Fibre Bragg grating
FE	Finite Elements
FH	Flight Hours
GVI	General Visual Inspection
LCC	Life Cycle Costing
MOL	Middle Of Life
NDT	Non-Destructive Techniques
NPV	Net Present Value
PFA	Probability of False Alarm
POD	Probability Of Detection
POF	Probability Of Failure
ROC	Receiver Operating Characteristic

2. INTRODUCTION

Maintenance represents a mandatory activity to maintain the proper level of safety in the aviation field, however, it requires not negligible resources in terms of manpower, spare parts and downtime costs. In airlines, maintenance can reach up to 28% of the operational costs Ref. 1. Currently, the maintenance tasks are carried out using NDT, like for instance tapping, ultrasounds, thermography, and radiography. Despite the effectiveness of such methods, they can be applied only locally, when the aircraft is on ground, and the component must be removed from the structure to be inspected. On the other hand, SHMS can provide an on-line monitoring of the component, and they are able to inspect the structure on a more diffused area compared to the classical NDT. The application of SHMS to aeronautical structures was deeply investigated in the literature. In Ref. 2 the authors investigated the performance of an FBG-based SHMS on a helicopter metallic stiffened panel for different crack lengths, in Ref. 3 the authors investigated the detection capability in a helicopter rotor blade through strain measurements, and in Ref. 4 Convolutional Neural Networks were used to recognize the presence of damages in a composite wing. Although such systems show some interesting aspects, especially related to the increase of the safety and the transition to the Condition-Based Maintenance, their economic impact on the lifecycle of the monitored structures remains still unclear. Some studies were presented in literature regarding this aspect, for instance in Ref. 1 the authors investigated the economic impact of Piezoelectric Wafer Active Sensor applied to the fuselage of a civil transportation aircraft, and concluded that no economic benefit would be obtained, as the saving in the maintenance cost would be compensated by the increase of the consumed fuel due to the extra weight of the SHMS. In Ref. 5 the SHMS was supposed replacing the phase of DVI related to A-check and C-check using piezoelectric sensors, the authors concluded that the equipment of the aircraft with a SHMS would have changed the aircraft performances, thus making the SHMS no more convenient. In Ref. 6 the authors investigated the effects of a SHMS on an Airbus A320 by using ultrasonic sensors and FBG sensors. The SHMS was supposed replacing the DVI and GVI. The authors concluded that an economic benefit would be achieved using the SHMS. In Ref. 7, a SHMS based on piezoelectric sensors was exploited to increase the allowable design values reducing the mass of the composite aircraft structure. It was found that the SHMS provides potential economic benefits in the structural components designed to be damage tolerant, while for the components designed for instability the SHMS provides no benefits.

Currently all the studies presented in literature are focused on aircraft Ref. 1, 5-10 and, to the best of the authors' knowledge, no studies were presented regarding the economic impact assessment of SHMS on helicopter's structural elements. Moreover, the studies focused only on the usage phase of the aircraft, neglecting the impact that the SHMS can have on the production and the development of structural elements. In this work, a procedure to assess the economic impact of SHMS was proposed, and the economic impact of an FBG-based SHMS was investigated on composite rotorcraft blades. The performance of the SHMS was assessed exploiting a FE model of the blade, which allowed simulating different damage scenarios to train the damage detection algorithm based on ANN. Both the lifecycle stages of BOL, corresponding to the production, and MOL, corresponding to the usage of the blade were investigated. The IDEF0 formalism allowed highlighting the key activities, input, outputs, resources and constraints at which each process was subjected. This allowed deriving the cost model. Two different scenarios were compared, according to the LCC methodology: the first, represented by the current situation in which the SHMS was not involved, in this work named "as is" scenario; while the second scenario was represented by the blade sensorized with FBG sensors, hereafter named scenario "with SHMS".

This work was organized as it follows: in section 3, the scenarios and the related cost models were presented, including the methodology adopted to derive the cost models in the two lifecycle stages (BOL and MOL); in section 4, the cost models were implemented, and a parametric results were presented for the BOL, while in the MOL the cost model was implemented in the Probabilistic Damage Tolerance Analysis. Eventually, in section 5, the conclusions and the main findings of the work were drawn.

3. Scenarios description and cost model definition

The lifecycle of all the products can be divided into three stages: (1) BOL, in which the component is produced and delivered to the market; (2) MOL, in which the component is employed and maintained by the customer to perform its operational functions; (3) EOL, in which the component is disposed. In this work, we focused on the first two lifecycle stages.

The following methodology was proposed to assess the economic impact of SHMS on the lifecycle of the rotorcraft: (i) identification of SHMS application; (ii) SHMS performance assessment; (iii) integration of SHMS in the lifecycle; (iv) Economic impact assessment. Accordingly with the step (i) of the procedure, the chosen structural element was represented by a composite rotorcraft blade sensorized with FBG sensors. The choice of the sensor was motivated by its immunity to the electromagnetic disturbances and its suitability to be embedded and protected into the laminate with a limited invasivity Ref. 11.

In the following subsections, more details were given concerning the other steps of the procedure.

3.1. Beginning Of Life

Regarding the step (ii) of the procedure to assess the economic impact of SHMS, the performance of the SHMS was not assessed for the BOL stage, as it would require an extensive experimental campaign, and it would be part of another work; while the step (iii) of the procedure, concerning the integration of the SHMS in the lifecycle of the rotorcraft, was hereby analyzed.

In the BOL stage, two main applications of the SHMS were considered regarding the laboratory activities to develop a new composite blade: the definition of the curing cycle, and the accomplishment of laboratory tests. The first was related to the development of the curing cycle, in such activity the distribution of the pressure and temperature over time of the curing cycle are found; the second corresponded to the accomplishment of laboratory tests needed to assess the structural integrity of the blade for the first stage of its certification. Currently, to find the right curing cycle for composite elements, a large number of curing cycles are needed, as the polymerization reaction of thermoset composites is known to be exothermic, and the temperature field inside the material is generally different from the one imposed by the autoclave. Nowadays the temperature of the material is measured by embedding some thermocouples in the laminate, and the proper curing cycle is found repeating the cycle adjusting the parameters until the desired temperature field in the material is reached. In the scenario "with SHMS", the SHMS was supposed to be employed in the development of the curing cycle by acquiring the temperature field during the autoclave cycle using the FBG sensors embedded in the blade and replacing the currently used thermocouples. The high accuracy of the measures obtained with the FBG sensors was supposed to provide a better accuracy of the temperature field inside the material, with the advantage to potentially save some of the curing cycles needed to find the proper cycle parameters. Once the curing cycle parameters are found, the next step consisted in the accomplishment of mechanical laboratory tests to analyze the mechanical properties of the blade. Currently this is obtained loading the blade with static and fatigue loads and measuring the strain using the strain gauges. In the scenario “with SHMS”, the SHMS was supposed replacing the strain gauges with FBG sensors, such to obtain a more accurate strain field, thus leading to a potential saving in the number of the mechanical tests performed in laboratory. The cost to perform the laboratory activities necessary develop a new composite blade can be split into two contributions, the first representing the cost to define the curing cycle, and the second representing the cost to perform the laboratory tests, as reported in Eq. 1.

$$C_{lab\ act} = C_{cur\ cycle\ def} + C_{test\ lab} \tag{1}$$

The process regarding the laboratory activities modeled with the IDEF0 formalism can be observed in Figure 1. The IDEF0 formalism is aimed at mapping complex processes with the scope to highlight following entities:

- Activities, represented in the rectangular boxes;
- Inputs, represented by the arrows entering from the left side of the activities;
- Outputs, represented by the arrows exiting from the right side of the activities;
- Constraints, represented by the arrows entering from the top side of the activities;
- Resources, represented by the arrows entering from the bottom side of the activities.

The cost models were derived considering the inputs and the resources required by all the activities involved in the process. The following color code convention was adopted: all the activities pertaining to the scenario “as is” were colored red, and the ones pertaining to the scenario “with SHMS” were colored green. The activities common to both the scenarios were colored black.

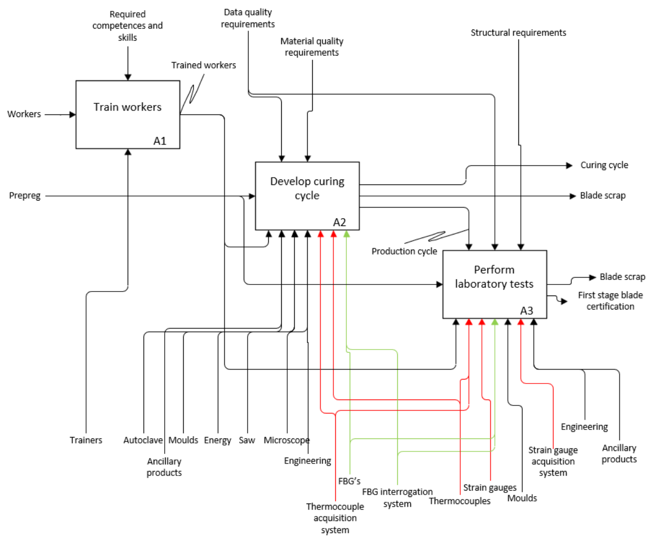

Figure 1: IDEF0 model of the process of the laboratory activities necessary to develop a new composite blade

Following the IDEF0 diagram, for the scenario “as is”, the following Eq. 2 representing the cost model for the development of the curing cycle can be obtained.

$$\begin{aligned} C_{cur\ cycle\ def}^{as\ is} = {} & \big(C_m + L_{tr\ wo} t_{tr\ wo} + n_{th} C_{th} \\ & + C_{energy} t_{auto} + L_{eng} t_{eng}\big) n_{auto}^{as\ is} \\ & + C_{acq\ sys} \frac{t_{auto} n_{auto}^{as\ is}}{t_{auto} n_{auto}^{as\ is} + t_{test} n_{test}^{as\ is}} \end{aligned} \tag{2}$$

While, considering the scenario “with SHMS”, the following Eq. 3 can be written.

$$\begin{aligned} C_{cur\ cycle\ def}^{SHMS} = {} & \big(C_m + L_{tr\ wo} t_{tr\ wo} + n_{FBG} C_{FBG} \\ & + C_{energy} t_{auto} + L_{eng} t_{eng}\big) n_{auto}^{SHMS} \\ & + C_{FBG\ sys} \frac{t_{auto} n_{auto}^{SHMS}}{t_{auto} n_{auto}^{SHMS} + t_{test} n_{test}^{SHMS}} \end{aligned} \tag{3}$$

The last term of Eq. 2 and Eq. 3 represented a cost partition of the acquisition system for the scenario “as is” and the interrogation system for the scenario “with SHMS”, respectively. It can be observed that both the equations are proportional to the number of autoclave cycles performed to find the proper curing cycle parameters. Moreover, it can be observed that the cost of the thermocouples in Eq. 2, regarding the scenario “as is” was replaced by the cost of the FBG sensors in Eq. 3, regarding the scenario “with SHMS”.

Regarding the activity of laboratory tests, necessary to complete the first stage of blade certification, the cost model for the scenario “as is” and for the scenario “with SHMS” is presented in Eq. 4 and Eq. 5, respectively.

$$C_{test\ lab}^{as\ is} = \left(C_m + L_{tr\ wo} t_{tr\ wo} + n_g C_g + C_{energy} t_{auto} + L_{eng} t_{eng}\right) n_{test}^{as\ is} + C_{acq\ sys} \frac{t_{test} n_{test}^{as\ is}}{t_{auto} n_{auto}^{as\ is} + t_{test} n_{test}^{as\ is}} \tag{4}$$

$$C_{test\ lab}^{SHMS} = \left(C_m + L_{tr\ wo} t_{tr\ wo} + n_{FBG} C_{FBG} + C_{energy} t_{auto} + L_{eng} t_{eng}\right) n_{auto}^{SHMS} + C_{FBG\ sys} \frac{t_{test} n_{test}^{SHMS}}{t_{auto} n_{auto}^{SHMS} + t_{test} n_{test}^{SHMS}} \tag{5}$$

The last term of Eq. 4 and Eq. 5 represented a cost partition of the acquisition system for the scenario “as is” and the interrogation system for the scenario “with SHMS”, respectively. It can be observed that both the equations are proportional to the number of blades tested. Moreover, it can be observed that the cost of the strain gauges in Eq. 4, regarding the scenario “as is” was replaced by the cost of the FBG sensors in Eq. 5, regarding the scenario “with SHMS”.

3.2. Middle Of Life

Following the step (ii) of the proposed procedure to assess the economic impact of SHMS, the performances of the SHMS were evaluated using an experimentally validated FE model representing part of the blade, more in specific the blade root. Damages were supposed occurring only in the adhesive layer connecting the central core to the surrounding anti-torsional layer. Different damage sizes were analyzed, ranging from 3 to 30 mm, and they were distributed over the adhesive’s surface colored red in Figure 2a. In the FE model, damages were obtained deleting the elements inscribed in a sphere whose center was located on the surface of the adhesive. An example of a damage of 30 mm size can be observed in Figure 2a. Two coordinate systems were used to locate the damages in the adhesive layer: a curvilinear coordinate and a cross-section coordinate. Damages were distributed in 10 equally spaced stations along the curvilinear coordinate and, for each of them, damages were also introduced in 4 evenly spaced stations in the cross-section coordinate. A total of 40 damage locations were analyzed. For each damage location the following sizes of damage were considered: 3, 6, 9, 12, 15, 18, 21, 24, and 30 mm, thus obtaining a total of 360 damage scenarios.

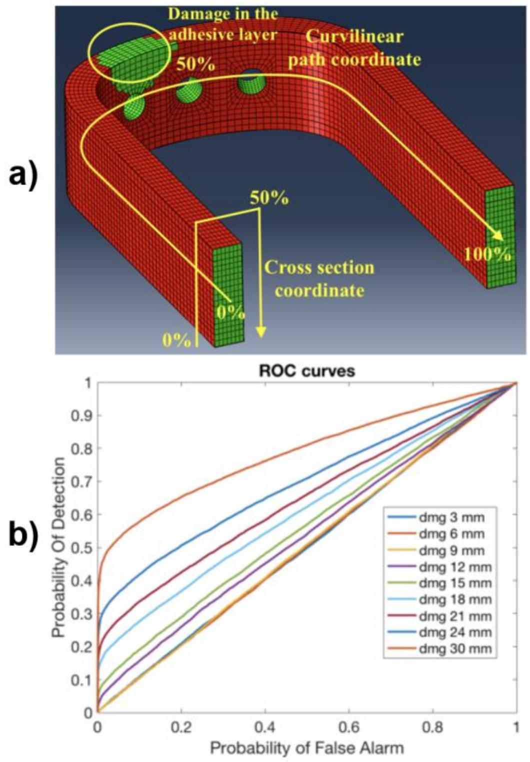

Figure 2: a) FE model of the blade root, the central core is colored green while the adhesive layer connecting the central core to the anti-torsional layer is colored red; b) Receiver Operating Characteristic curve obtained for a Gaussian noise of 4%.

The analyses served as input to train an algorithm based on ANN, which detected the presence of damages. Strain measurements were taken by some of the elements of the model and considering 6 virtual lines of optical fibres with 10 virtual FBG’s for each one, for a total of 60 virtual FBG sensors located inside the anti-torsional layer at a distance of 0.25 mm from the adhesive layer. A Gaussian noise of 4% was then introduced in the sampled strain values during the training, validation and test of the ANN. An ANN for pattern recognition having 3 hidden layers and 10 neurons per layer was adopted to detect the presence of damages: since the output was a scalar number between 0 and 1, the blade was considered damaged if the output of the ANN exceeded a certain threshold, otherwise it was considered undamaged. The damage detection performances of the SHMS were obtained in terms of POD and PFA, presented in Figure 2b, for a Gaussian noise level of 4%. The ROC curves were obtained varying the threshold between 0 and 1, and the POD was obtained dividing the number of damaged blades classified as damaged by the total number of damaged blades in input to the ANN, while the PFA was obtained dividing the number of undamaged blades classified as damaged by the total number of undamaged blades given in input to the ANN.

The step (iii), concerning the integration of the SHMS in the lifecycle of the rotorcraft is hereby presented.

In both the scenarios, “as is” and “with SHMS”, to account for the loss of revenue due to the downtime of the machine, the helicopter was supposed to be owned by a company renting its helicopters to other companies. Considering the scenario “as is”, and based our experience in the aerospace field, the blade was supposed to be subjected to two types of inspections: GVI, supposed to be performed every 50 FH without removing the blade from the rotor hub, and DI, supposed to be performed with the tap hammer every 1200 FH removing the blade from the rotor hub. The yearly cash flow for the scenario “as is” can be expressed by Eq. 6.

$$CF^{as\ is} = \sum_{i=1}^{n\ travels} 2At_{depot}K_{partition} + \sum_{i=1}^{n\ blade\ mount-sched} 2Bt_{mount\ blade} + \sum_{i=1}^{n\ blade\ mount-unsch} \frac{2}{n_b}Ct_{mount\ blade} + \sum_{i=1}^{n\ GVI} Bt_{GVI} + \sum_{i=1}^{n\ DI} Bt_{DI} + \sum_{i=1}^{n\ repairs} Ct_{repair}^{as\ is} + \sum_{i=1}^{n\ spare\ parts} c_{blade}^{as\ is} \tag{6}$$

Where the coefficients A, B, and C were defined by the Eq. 7, Eq. 8, and Eq. 9, respectively.

$$A = \left(L_{pilots} + c_{fuel} + R\right) \tag{7}$$

$$B = \left(L_{tr\ wo} + RK_{partition}\right) \tag{8}$$

$$C = \left(L_{tr\ wo} + R\right) \tag{9}$$

Different cost elements were considered: the cost to travel to the depot, the cost to remove the blade from the rotor hub, the cost to perform GVI and DI, the cost to repair the blade, and the cost to substitute the blade. It can also be observed that a distinction was made between scheduled and unscheduled activities. In the scheduled activities, the partition coefficient $K_{partition}$ was introduced with the scope to allocate the loss of revenue R to the activities related to the blade, more in detail, if the helicopter is on ground, and other maintenance tasks are performed at the same time, the portion of revenue loss related to the maintenance of the blade represents only a part of the revenue loss due to the other maintenance activities on the helicopter. On the contrary, this is not true for the unscheduled activities generated by the rotor blades: in this case, since the activities are not carried out according to a schedule, the other maintenance tasks related to other structural elements out of the blade cannot be carried out in parallel. Therefore, the revenue loss R generated by the rotor blades’ activities cannot be partitioned. As a consequence, it is expected that the unscheduled activities are costlier than the scheduled ones.

In the scenario “with SHMS”, the GVI was supposed to be carried out at the same way as for the scenario “as is”, while the SHMS was supposed to gradually replace the DI: in the first years of the lifecycle, the interval of the DI was supposed to be extended up to 2400 FH thanks to the automatic scheduled inspections performed in addition with the SHMS. In the last years of the lifecycle, when the confidence in the performance of the SHMS was increased, the SHMS was supposed to completely replace the DI, so achieving a pure Condition-Based Maintenance. It must be specified that the SHMS was supposed to be interrogated at scheduled time intervals by an operator on the ground. However, upon advice provided by the SHMS, if the GVI did not evidence any damage, the helicopter was supposed to fly back to the depot to perform the DI with the same methodology adopted for the scenario “as is”. The yearly cash flow for the scenario “with SHMS” can be expressed by Eq. 10.

$$
\begin{aligned}
CF^{SHMS} = & \sum_{i=1}^{n\,travels-sched} 2At_{depot}K_{partition} \\
& + \sum_{i=1}^{n\,travels-unsch} 2At_{depot} \\
& + \sum_{i=1}^{n\,blade\,mount-sched} 2Bt_{mount\,blade} \\
& + \sum_{i=1}^{n\,blade\,mount-unsch} \frac{2}{n_b}Ct_{mount\,blade} \\
& + \sum_{i=1}^{n\,GVI-sched} Bt_{GVI} \\
& + \sum_{i=1}^{n\,GVI-unsch} \frac{1}{n_b}Ct_{GVI} \\
& + \sum_{i=1}^{n\,DI-sched} Bt_{DI} + \sum_{i=1}^{n\,DI-unsch} \frac{1}{n_b}Ct_{DI} \\
& + \sum_{i=1}^{n\,repairs} Ct_{repair}^{SHMS} \\
& + \sum_{i=1}^{n\,spare\,parts} c_{blade}^{SHMS}
\end{aligned}
\qquad (10)
$$

It can be observed that a different cost for the blade and for the repairing time was assumed with respect to the scenario “as is”. Moreover, the travel activity was supposed to be also unscheduled, differently from the “as is” scenario, since an advice of the SHMS would lead the helicopter travelling to the depot for a DI.

The NPV, presented in Eq. 11, was chosen as performance index to compare the two scenarios, which allowed actualizing all the cash flows occurring during the usage of the helicopter in its lifecycle.

$$
NPV = \sum_{t} \frac{CF(t)}{(1+r)^t} \qquad (11)
$$

The two scenarios, “as is” and “with SHMS”, were compared at the same level of POF of the blade, which was obtained implementing the probabilistic damage tolerance analysis Ref. 13. According to Ref. 14, a helicopter is subjected to an impact event with the main rotor once every 1000 FH in an offshore environment, and considering an average of 500 FH per year for 30 years of life, a total of 15 impacts are expected in the whole lifecycle of a helicopter, which were distributed randomly in the simulation of the lifecycle. The impact energies were distributed according to Ref. 15 considering the “medium energy”. The blade degradation after an impact was assumed to be similar to the one presented in Ref. 16, in which a helicopter blade was subjected to impacts with steel spheres at different energies, and the residual indentation, and the skin-foam disbonding area were given. The residual strength of the blade after an impact was estimated considering the ratio between the cross-sectional area affected by the indentation, and the initial cross-sectional area. A schematic representation of the blade strength degradation can be observed in Figure 3a.

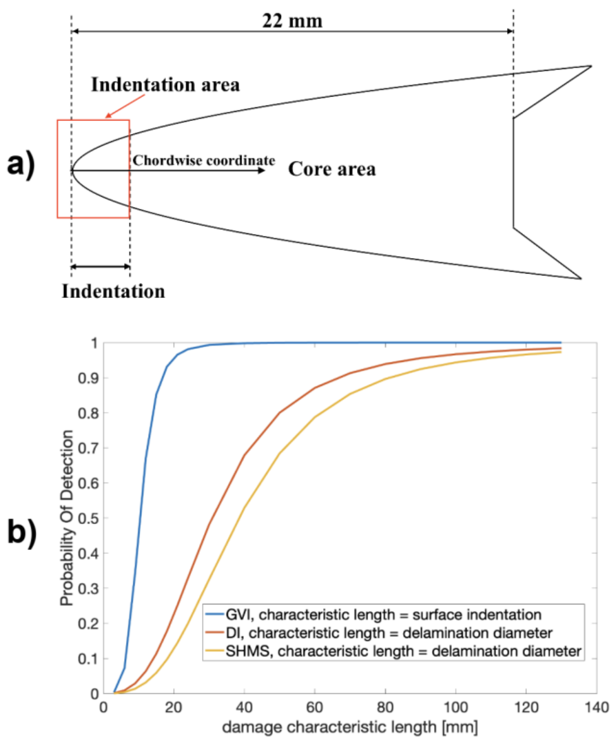

Figure 3: a) Schematic representation of the blade strength degradation function of the residual indentation; b) POD curves corresponding to the GVI, DI, obtained from Ref. 17, and SHMS, the latter calculated considering a threshold such to reach a PFA of 0.12% from the ROC curves presented in Figure 2b.

Accordingly, the following Eq. 12 was used to compute the ratio between the initial strength and the strength after an impact.

$$
strength\ ratio = 1 - 1.5\frac{indentation\ area}{core\ area} \qquad (12)
$$

Where the coefficient equal to 1.5 was introduced to consider the stress concentration effects. The indentation area was calculated assuming the shape of the cross section close to the leading edge well approximated by the square root function, thus obtaining Eq. 13, which provided the indentation area function of the indentation depth.

$$indentation\ area\ = 2.89 \times indentation^{1.5} \qquad (13)$$

Figure 3b shows the performance of the GVI, DI, and SHMS in terms of POD function of the damage size. It must be remarked that, while for DI and SHMS the damage size was represented by the delamination size, for the GVI the characteristic length was represented by the surface indentation. GVI and DI curves were obtained from Ref. 17, while the performance of the SHMS were previously obtained exploiting the FE model of the blade root, and assuming that the obtained performances were representative of the whole length of the blade. Accordingly, assuming the length of the blade being 7.5 the length of the portion analyzed with the FE model, the number of FBG sensors in one blade were scaled linearly, and a total of 450 FBG sensors for one blade was considered.

In the Probabilistic Damage Tolerance Analysis, the load exceedance probability per FH was calculated according to Ref. 18, and the initial blade strength ratio was set to 2, which represented the ratio between the failure load and the limit load. The lifecycle of the blade was simulated hour by hour, and it was implemented in a Matlab script: the POF of the blade was averaged on 30000 simulated scenarios. Hour by hour, the code checked if the time to perform an inspection was reached, therefore the inspection intervals of GVI, DI, and SHMS (the latter only for the scenario “with SHMS”) represented an input of the code. The cost model presented by the Eq. 6-11 was implemented in the code, which summed up the cash flows for each year of the lifecycle and at the end computed the NPV.

4. Results

In this section, the last step (iv) of the procedure to assess the economic impact of SHMS was accomplished.

In Table 1, some values of the variables adopted to assess the economic impact in this study were reported.

Table 1: values and sources of the variables assumed in this study.

Variable	Value	Source
$C_{acq\ sys}$	13000 €	Ref. 19
$c_{blade}^{as\ is}$	40000 €	DAER-lab
C_{energy}	10.6 €/h	Ref. 20
C_{FBG}	90 €	DAER-lab
$C_{FBG\ sys}$	20000 €	Ref. 21
c_{fuel}	272.64 €/h	Ref. 22, 23
C_g	1 €	DAER-lab
C_m	1307 €	Ref. 20 and DAER-lab
C_{th}	10 €	Ref. 24
$K_{partition}$	0.1	DAER-lab
L_{eng}	42 €/h	DAER-lab
L_{pilots}	48.2 €/h	Ref. 25
$L_{tr\ wo}$	28 €/h	Ref. 26
n_b	4	DAER-lab
n_{FBG}	450	DAER-lab
R	6560.6 €/h	Ref. 27
r	8%	Ref. 28
t_{auto}	8 h	DAER-lab
t_{depot}	0.5 h	DAER-lab
t_{DI}	15 h	DAER-lab
t_{eng}	0.0167 h	DAER-lab
t_{GVI}	0.652 h	DAER-lab
$t_{mount\ blade}$	0.5 h	DAER-lab
$t_{repair}^{as\ is}$	8 h	DAER-lab
$t_{tr\ wo}$	25 h	DAER-lab

4.1. Beginning Of Life

The results concerning the BOL pointed out the presence of break-even points, across which one of the two scenarios become more convenient than the other one.

Regarding the development of the curing cycle, it was found that if the number of curing cycles to find the proper curing parameters is reduced enough thanks to the higher quality of the temperature field obtained with the FBG sensors, then an economic benefit can be achieved, and the scenario “with SHMS” resulted to be more convenient. For instance, it can be observed from Figure 4a, that if the number of curing cycles is reduced from 26, in scenario “as is”, to a number below 19 using 10 FBG sensors (scenario “with SHMS”), then an economic benefit is achieved by the scenario “with SHMS”.

Regarding the laboratory tests necessary for the first stage of blade certification, an analogous result was found. Some break-even points were found across which one of the two scenarios become more convenient than the other one. It was found that if a sufficient reduction of the number of tested blades is reached thanks to the higher quality of the strain field obtained with the FBG sensors, then an economic benefit can be achieved in the scenario “with SHMS”. For instance, considering the result shown in Figure 4b, if the number of tested blades (number of laboratory tests) is reduced from 22, in the scenario “as is”, below 18, in the scenario “with SHMS” using 10 FBG sensors, then an economic benefit is achieved.

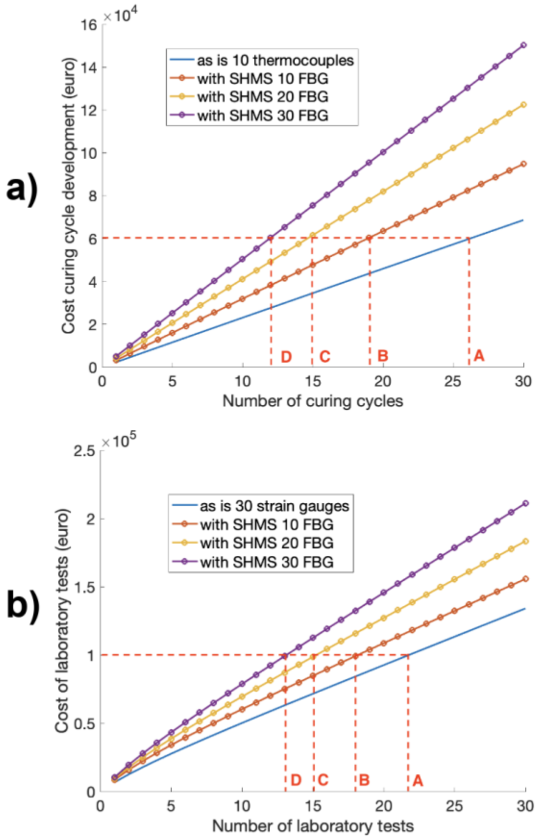

Figure 4: a) Cost of the curing cycle development versus the number of curing cycles performed, with sensitivity analysis on the number of FBG sensors embedded in the blade; b) Cost of laboratory tests versus the number of laboratory tests (tested blades), with sensitivity analysis on the number of FBG sensors embedded in the blade.

4.2. Middle Of Life

The results concerning the MOL suggested that in the scenario “with SHMS” was possible to increase the DI interval up to 2400 FH if automatic inspections with the SHMS every 1070 FH were performed in addition to maintain the same POF of the blade. For such a reason, the comparison between the two scenarios was done considering an automatic inspection interval of the SHMS equal to 1070 FH: as it can be observed in Figure 5, such condition corresponds to the green vertical dashed line. Comparing the two scenarios in correspondence of that line, a negative economic impact of the SHMS on the lifecycle of the helicopter was found. Referring to Figure 5, the points A and B, corresponding to the scenario “as is” and “with SHMS”, respectively, the NPV for the scenario “as is” corresponded to 1.89×10^5€, while the NPV for the scenario “with SHMS” corresponded to 2.726×10^5€. This means that the maintenance of the helicopter in the scenario “with SHMS” resulted to be more expensive with respect to the scenario “as is”.

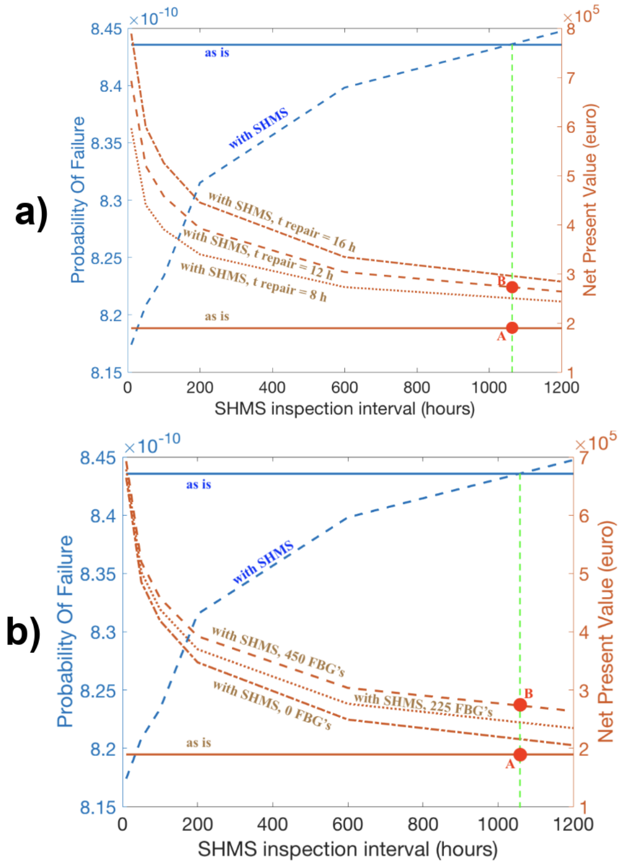

Figure 5: a) POF and NPV function of the inspection interval of the SHMS, with sensitivity analysis on the repairing time of the sensorized blade; b) POF and NPV function of the inspection interval of the SHMS, with sensitivity analysis on the number of FBG sensors charged to the customer.

One of the reasons lies in the large number of unscheduled activities generated by the SHMS, which make difficult synchronizing the maintenance activities, so increasing the helicopter downtime. Observing the partition of the NPV, it was found that a reduction in the effort of the DI was achieved using the SHMS, passing from 22% in the scenario "as is" to 6% in the scenario "with SHMS". However, the obtained saving was compensated by a higher cost of the spare parts and the repairing operations.

It is also interesting to observe the results of the sensitivity studies presented in Figure 5a and Figure 5b, where it is shown that even considering the same repairing time of 8 h for the two blades (standard and sensorized), the scenario more convenient remained the scenario "as is". Even considering the hypothesis in which the cost of the FBG sensors was not charged to the customer, corresponding to Figure 5b, the scenario more convenient remained the scenario "as is".

5. CONCLUSIONS

In this work, the economic impact of an FBG-based SHMS was investigated under two perspectives: BOL and MOL. The assessment was performed exploiting the LCC methodology, which prescribed to compare different alternatives. In this study, two different alternatives were compared, one was represented by the scenario "as is", and the other was represented by the scenario "with SHMS". Overall, the following conclusions can be drawn from the results presented in the paper, and they are hereby reported:

1. A methodology to assess the economic impact of SHMS was presented, which was applied to the case of a rotorcraft composite blade, but it can be generalized and adapted to other composite structural elements;
2. An application of the SHMS was proposed in the BOL stage, and it was found that a positive economic impact can be reached if a sufficient number of autoclave cycles and tested blades are saved in the process of curing cycle definition and accomplishment of laboratory tests, respectively;
3. The application of the SHMS to the composite rotorcraft blade in the MOL stage shown a negative economic impact, as it was found that the saving obtained with the automatic scheduled inspection performed with the SHMS were compensated by a higher cost of the spare parts and a higher effort in the repairing operation.
4. To make the SHMS cost-effective, they should be applied to the right structural elements, represented by the components difficult to reach during the maintenance operations, such that the potential of the SHMS could be fully exploited.

Future works should be carried out to quantify the actual reduction of the number of curing cycles and of the number of laboratory tests as a consequence of a higher quality of the temperature field and the strain field obtained with the FBG sensors.

Author contacts:

Pietro Ballarin pietro.ballarin@polimi.it

Giuseppe Sala giuseppe.sala@polimi.it

Marco Macchi marco.macchi@polimi.it

Irene Roda irene.roda@polimi.it

Andrea Baldi andrea.baldi01@leonardo.com

Alessandro Airoldi alessandro.airoldi@polimi.it

6. REFERENCES

1. Dong, T., & Kim, N. H. (2018). Cost-effectiveness of structural health monitoring in fuselage maintenance of the civil aviation industry. *Aerospace, 5(3)*, 87.
2. Sbarufatti, C., Manes, A., & Giglio, M. (2013). Performance optimization of a diagnostic system based upon a simulated strain field for fatigue damage characterization. *Mechanical Systems and Signal Processing, 40(2)*, 667-690.
3. Serafini, J., Bernardini, G., Porcelli, R., & Masarati, P. (2019). In-flight health monitoring of helicopter blades via differential analysis. *Aerospace Science and Technology, 88*, 436-443.
4. Lin, M., Guo, S., He, S., Li, W., & Yang, D. (2022). Structure health monitoring of a composite wing based on flight load and strain data using deep learning method. *Composite Structures*, *286*, 115305.
5. Cusati, V., Corcione, S., & Memmolo, V. (2021). Impact of structural health monitoring on aircraft operating costs by multidisciplinary analysis. *Sensors*, *21*(20), 6938.

6. Büchter, K. D., Sebastia Saez, C., & Steinweg, D. (2022). Modeling of an aircraft structural health monitoring sensor network for operational impact assessment. *Structural Health Monitoring*, *21*(1), 208-224.
7. Dienel, C. P., Meyer, H., Werwer, M., & Willberg, C. (2019). Estimation of airframe weight reduction by integration of piezoelectric and guided wave–based structural health monitoring. *Structural Health Monitoring*, *18*(5-6), 1778-1788.
8. Cusati, V., Corcione, S., & Memmolo, V. (2022). Potential benefit of structural health monitoring system on civil jet aircraft. *Sensors*, *22*(19), 7316.
9. Steinweg, D. M., Hornung, M., & Bauhaus Luftfahrt eV, W. (2019). *Methods evaluating the impact of structural health monitoring on aircraft lifecycle costs*. Bonn, Germany: Deutsche Gesellschaft für Luft-und Raumfahrt-Lilienthal-Oberth eV.
10. Boller, C. (2014). Implementation Strategies for SHM in Civil and Military Applications. *Structural Health Monitoring of Military Vehicles; Suleman, A., Ed.; STO-EN-AVT-220. STO Educational Notes*.
11. Sala, G., Di Landro, L., Airoldi, A., & Bettini, P. (2015). Fibre optics health monitoring for aeronautical applications. *Meccanica*, *50*, 2547-2567.
12. Bottasso, L. M., Sala, G., Bettini, P., Tagliabue, P., Corbani, F., Platini, E., Guerra, A., Anelli, A. (2018). Rugged Fiber Optics Monitoring System for Helicopter Rotor Blades. In *44th European Rotorcraft Forum (ERF 2018)* (pp. 965-980). Curran Associates.
13. Palmberg, B., Blom, A. F., & Eggwertz, S. (1987). Probabilistic damage tolerance analysis of aircraft structures. In *Probabilistic fracture mechanics and reliability* (pp. 47-130). Dordrecht: Springer Netherlands.
14. Weber, S., Lone, M., & Cooke, A. (2019). Recent experiences of helicopter main rotor blade damage. *Journal of the American Helicopter Society*, *64*(3), 1-5.
15. Kan, H. P. (1998). *ENHANCED RELIABILITY PREDICTION METHODOLOGY FOR IMPACT DAMAGED COMPOSITE STRUCTURES* (No. DOT/FAA/AR-97/79).
16. Tawk, I., Aubry, J., Navarro, P., Ferrero, J. F., Marguet, S., Rivallant, S., ... & Rauch, P. (2012). Study of impact on helicopter blade. *Engineering Failure Analysis*, *24*, 38-45.
17. Huang, C., & Lin, K. (2005, April). A method for reliability assessment of aircraft structures subject to accidental damage. In *46th AIAA/ASME/ASCE/AHS/ASC Structures, Structural Dynamics and Materials Conference* (p. 1830).
18. Chen, X., Ren, H., Bil, C., & Cai, J. (2014). Repair tolerance analysis for composite structures using probabilistic methodologies. *Journal of Aircraft*, *51*(6), 1997-2004.
19. Cost of acquisition system. Accessed on 10th of July 2023. Url: https://b2bstore.hbm.com/myHBM/app/displayApp/(cpgnum=1&layout=7.01-16_153_6_9_70_34_65_73_134_6&uiarea=6&citem=CC58514E6AD90F12E1000000AC1099340017A47744441EE1B2B08ED8335B1888&carea=CC58514E6AD90F12E1000000AC109934&rdb=0&cpgsize=0)/.do?rf=y.
20. Morse, L., Cartabia, L., & Mallardo, V. (2022). Reliability-based bottom-up manufacturing cost optimisation for composite aircraft structures. *Structural and Multidisciplinary Optimization*, *65*(5), 159.
21. Cost of interrogation system. Accessed on 10th of July 2023. Url: https://b2bstore.hbm.com/myHBM/app/displayApp/(cpgnum=1&layout=7.01-16_153_6_9_70_34_65_73_134_6&uiarea=6&citem=319DCC4F1E60564AE1000000AC109A0CA01D4895C9E81EE79BC34A9F7F62510B&carea=319DCC4F1E60564AE1000000AC109A0C&xcm=hbm_b2boccasionalcrm&rdb=0&cpgsize=0)/.do?rf=y
22. Cost of fuel. Accessed on 23rd of July, 2023. Url: https://jet-a1-fuel.com/price/italy.
23. Fuel consumption. Accessed on 22nd of July, 2023. url: http://c.eqcdn.com/_a15f1bfe5225ae94a025b%204998691df71/%20ergrpinc/db/61/472/spec_sheet/AW139+Spec+Sheet_09_16_2016.pdf.

24. Cost of thermocouples. Accessed on 10th of July,2023. Url: https://www.ersa-shop.de/de/product_info.php?info=p1912_themoelement-k-type.html&gad=1&gclid=EAIaIQobChMIyZ3T4q-DgAMVqItoCR2UhACiEAQYDSABEgL8D_D_BwE.
25. Labour rate helicopter pilots. Accessed on 25th of October, 2023. url: https://ca.indeed.com/q-helicopter-pilot-jobs.html.
26. Labour rate aircraft maintenance technicians. Accessed on 25th of October, 2023. url: https://www. indeed.com/career/aircraft-maintenance-technician/salaries.
27. Annual revenue. Accessed on 22nd of July, 2023. url: https : / / www . statista . com / statistics /629751/babcock-international-annual-revenues/.
28. Discount rate. Accessed on 16th of July, 2023. url: https://valueinvesting.io/BAB.L/valuation/wacc.